Received: 19 March 2024 | Revised: 26 September 2024 | Accepted: 1 October 2024

DOI: 10.1002/pld3.70018

RESEARCH ARTICLE

The *BnaBPs* gene regulates flowering time and leaf angle in *Brassica napus*

Jiang Yu[1] | Yi-Xuan Xue[1] | Rehman Sarwar[1] | Shi-Hao Wei[2] | Rui Geng[1] | Yan-Feng Zhang[2] | Jian-Xin Mu[2] | Xiao-Li Tan[1]

[1]School of Life Sciences, Jiangsu University, Zhenjiang, Jiangsu, China

[2]Hybrid Rape Research Center Shaanxi Prov, Yangling, Shanxi, China

Correspondence
Xiao-Li Tan, School of Life Sciences, Jiangsu University, Zhenjiang 212013, Jiangsu, China.
Email: xltan@ujs.edu.cn

Funding information
Jiangsu Agricultural Science and Technology Innovation Fund (JASTIF), Grant/Award Number: CX (21) 2009; JST | Jiangsu Provincial Key Research and Development Program (Key Technologies R&D Program of Jiangsu Province), Grant/Award Numbers: BE2023342, BE2022340

Abstract

The flowering time and plant architecture of *Brassica napus* were significantly associated with yield. In this study, we found that the *BREVIPEDICELLUS/KNAT1*(*BP*) gene regulated the flowering time and plant architecture of *B. napus*. However, the precise regulatory mechanism remains unclear. We cloned two homologous *BP* genes, *BnaBPA03* and *BnaBPC03*, from *B. napus* Xiaoyun. The protein sequence analysis showed two proteins containing conserved domains KNOX I, KNOX II, ELK, and HOX of the KONX protein family. The CRISPR/Cas9 knockout lines exhibited early budding and flowering time, coupled with floral organ abscission earlier and a larger leaf angle. On the contrary, overexpression plants displayed a phenotype that was the inverse of these characteristics. Furthermore, we observed upregulation of gibberellin and ethylene biosynthesis genes, as well as floral integrator genes in knocked-out plants. The results revealed that *BnaBPs* play a role in flowering time, floral organ abscission, and leaf angle as well as germination processes mediated. Additionally, *BnaBPs* exerted an impact on the biosynthesis pathways of ethylene and GA.

KEYWORDS
BnaBP, *Brassica napus*, flowering time, KNOX protein family, plant architecture

1 | INTRODUCTION

B. napus (AACC, $n = 19$) is a naturally occurring interspecific hybrid that maintains diploidy, resulting from the union of *Brassica rapa* (AA, $n = 10$) and *Brassica oleracea* (CC, $n = 9$). The *B. napus* cultivar exhibits a remarkable capacity for high seed and oil yields, establishing it as the predominant oil-producing *Brassica* crop worldwide (Lu et al., 2019). In addition, it is rich in essential nutrients such as vitamins, sterols, and other beneficial components that are highly desired by consumers in various industries (Beyzi et al., 2019; Ye & Liu, 2023). In recent years, while rapeseed production has remained relatively stable with a slight increase, it still heavily relies on imports. Consequently, enhancing the yield of rapeseed has immense importance in ensuring the secure supply of edible oil in China.

The regulation of plant architecture and phenology plays a crucial role in plant productivity and is intricately associated with yield (Wang et al., 2018). The optimal planting density of the crops was determined by factors such as the angle of the leaf and the angle of the branch, which had a direct impact on photosynthetic efficiency and ultimately yield (Donald, 1968). The attached petals can prevent the further spread of *Sclerotinia sclerotiorum* from the petals to the leaves and reduce the damage caused by stem rot disease (Geng et al., 2022).

JiangYu and Yi-Xuan Xue contributed equally to this work.

Variations in flowering times between plants were the result of their adaptations to competitive pressures for pollination and diverse climatic conditions. Early blooming of crops indicates a shorter reproductive development cycle, ultimately leading to increased yields (Song et al., 2010). Plant growth and development were governed by intricate regulatory networks, in which hormone production and distribution serve as key signaling molecules. The determination of plant architecture and flowering time was a consequence of continuous modifications in the growth and development cycle of plants, which were influenced by various hormonal factors. For instance, in the context of rice, gibberellin (GA) treatment induced degradation of the DELLA protein SLENDER RICE 1 (SLR1), a crucial inhibitory factor within the GA signaling pathway, while failing to impede the degradation of MONOCULM 1 (MOC1), a pivotal protein involved in rice tillering formation. Consequently, this led to a reduction in tiller count and an increase in plant height (Liao et al., 2019). The flowering time of plants was influenced by multiple signaling pathways, among which the GA pathway holds significant importance. GA can facilitate the degradation of the DELLA protein via the ubiquitination pathway, thereby repressing downstream flowering genes such as *FLOWERING LOCUS T* (*FT*) and *SUPPRESSOR OF OVEREXPRESSION OF CONSTANS1* (*SOC1*) to promote flowering (Fukazawa et al., 2021). Moreover, the shedding of plant organs is significantly influenced by the balance between ethylene and auxin (Cheng et al., 2022; Taylor & Whitelaw, 2001).

The *KNOX* gene family plays a pivotal role as a transcription factor in the regulation of plant growth and development, encompassing four distinctive domains, namely, KNOX I, KNOX II, ELK, and HOX. This gene family is primarily categorized into two subfamilies known as KNOXI and KNOXII. In Arabidopsis, the identified *KNOX* genes were classified into two classes: *KNOX I*, which included *SHOOT-MERISTEMLESS* (*STM*), *BREVIPEDICELLUS/KNAT1* (*BP*), *KNAT2*, *KNAT6*, and *KNOX II*, which includes *KNAT3*, *KNAT4*, *KNAT5*, and *KNAT7*. Notably, the absence of the HOX domain distinguishes the separate classification of *KNATM* (Magnani & Hake, 2008). The BP protein, classified as a Class I KNOX transcription factor, plays a pivotal role in maintaining the activity of the stem apex meristem and regulating the initiation and separation of lateral organs (Long et al., 1996; Ragni et al., 2008). The active expression of *BP* was also observed in the pedicels, intersegmental cortex, and meristem of bud tips (Douglas et al., 2002). Meanwhile, *BP* has been shown to exert regulatory effects on plant architecture and hormone homeostasis in various species, including tomato (Meir et al., 2010), Arabidopsis (Lincoln et al., 1994), rice (Yoon et al., 2017), and litchi (Zhao et al., 2020). Specifically, it modulates enzymes involved in the GA and ethylene biosynthesis pathways, such as GA-20 oxidase (GA20ox), 1-aminocyclopropane-1-carboxylate synthase (ACS), and ACC oxidase (ACO). However, despite extensive research on the regulation of plant morphology and hormone levels by *BP* in model plants, there remain numerous knowledge gaps in rapeseed.

In this study, we investigated the biological function of *BnaBP* by overexpression and gene-knockout lines in *B. napus*, elucidating the impact of *BnaBP* on flowering time and plant architecture. Our findings aim to provide a theoretical foundation for breeding new germplasm with the desired plant architecture and flowering time, thus contributing to advances in crop improvement.

2 | MATERIALS AND METHODS

2.1 | Materials

In this study, the spring *B. napus* Xiaoyun was utilized as the parental material for both wild type (WT) and genetically transformed plants (Wang et al., 2024). Generation of bp mutants (*bp2-11*, *bp1-8*, *bp1-11*, *bp1-13*, *bp1-31*, and *bp1-33*) was achieved through CRISPR/Cas9 technology (see below). Simultaneously, overexpressed plants (OE-12, OE-15, and OE-16) were generated by transforming the 35S::*BnaBPA03*-eGFP vector (see below). All plants were cultivated under controlled conditions in a culture chamber with a constant temperature of (20 ± 2)°C, a light cycle of 16 h on and 8 h off, a light intensity of 480 $mol \cdot m^{-2} \cdot s^{-1}$, and a relative humidity ranging from 60% to 70% (Guo et al., 2017).

2.2 | Reconstruction of phylogenetic trees and analysis of conserved domains

To obtain Class I and Class II *KNOX* protein sequences (Bueno et al., 2020), we retrieved data from the Arabidopsis database (https://www.arabidopsis.org/index.jsp), Subsequently, their homologous proteins were retrieved from the *B. napus* database (https://yanglab.hzau.edu.cn/BnGDXY/#/) and the rice database (https://www.ricedata.cn/). Subsequently, we employed the Align by Muscle tool in Molecular Evolutionary Genetics Analysis Version 5 (MEGA5) for aligning the previously obtained protein sequences and saved the output as a file in MEGA format. The resulting sequence alignment file was then imported to construct a maximum likelihood phylogenetic tree with 1000 bootstrap replications using default parameters (Tamura et al., 2011). The conserved domains of KNOX family proteins in *B. napus*, Arabidopsis, and *Oryza sativa* were analyzed using the NCBI protein Domain search tool Conserved Domain (https://www.ncbi.nlm.nih.gov/Structure/cdd/wrpsb.cgi) with default parameters. The resulting structures were visualized using Tbtools (Chen, Chen, et al., 2020).

2.3 | Vector construction, gene transformation, and identification of transgenic plants

We designed four target sequences that are all capable of simultaneously targeting the genes *BnaBPA03* and *BnaBPC03* using CRISPR-P2.0 (http://crispr.hzau.edu.cn/CRISPR2/). Following the methodology proposed by Xing et al. (2014), target sequence 1 and target sequence 3 were ligated to the pKSE401 vector backbone, resulting in the construction of the PKSE401-*BnaBP*-1 vector.

Similarly, target sequence 2 and target sequence 4 were connected to the pKSE401 vector backbone to generate the PKSE401-*BnaBP*-2 vector. The target sequences are presented in Table S1. To construct the *35S::BnaBPA03*-eGFP construct, the complete CDS sequence of *BnaBPA03* was amplified with the primers BnaBPCDS-F/R using the total cDNA obtained from inflorescence tip tissue of the Xiaoyun rapeseed cultivar as a template. The *35S::BnaBPA03*-eGFP plasmid was constructed using Gateway cloning technology. The coding region of *BnaBPA03* without the stop codon was PCR amplified using primers 2.0A03-F/R. The PCR products were cloned into the pENTR vector using the PENTR™/D-TOPO™ Cloning Kit according to the manufacturer's instructions (Invitrogen, China) and the resulting Gateway entry clones were then cloned into the destination vector pK7FWG2.0 to create a C-terminal GFP fusion using the Gateway LR recombinase. The gene editing vector and overexpression vector were introduced into *B. napus* Xiaoyun through plant tissue culture technique and *Agrobacterium* (GV3101)-mediated genetic transformation method (Bhalla & Singh, 2008; Wang et al., 2024). The target sequences of *BnaBPA03* and *BnaBPC03* genes in knockout plants were amplified using primer sets BnaBPA03Gen-F/R and BnaBPC03Gen-F/R, respectively. Subsequently, Sanger sequencing was performed to obtain the sequence data for the knockout plants. We utilized BnaBP-QF/R as a primer, employed WT plants as the control group, and used the 35S::*BnaBPA03*-eGFP vector to transform plant leaf cDNA as a template. Subsequently, we performed RT qPCR (refer to below) in order to identify overexpressed plants. We tabulated the serial number of plants in which editing occurred within the target sequences of *BnaBPA03* and *BnaBPC03* genes, along with the corresponding editing types, as illustrated in Figure S1. Additionally, we successfully obtained three *B. napus* plants overexpressing *BnaBPA03*, designated as OE-12/15/16 (Figure S2c).

2.4 | Analysis of subcellular localization

Observation of subcellular localization through protoplast preparation: The fusion expression of BnaBPA03 and GFP was achieved using the 35S::*BnaBPA03*-eGFP vector, which was employed to observe the subcellular localization of BnaBPA03. The leaves used for protoplast preparation were derived from rapeseed plants that had been stably transformed with the 35S::*BnaBPA03*-eGFP vector through plant tissue culture technique and *Agrobacterium* (GV3101)-mediated genetic transformation method (refer to above), and the leaf veins were removed and cut into small pieces (approximately 4–5 mm). The chopped leaves were placed into a syringe containing 2 mL of cell wall digestion solution and subjected to repeated pressurization. The cell wall digestion solution, along with the leaf pieces, was then transferred to a 2 mL EP tube and digested at 24°C for 2 to 4 h, with gentle inversions performed every hour. After digestion, the leaf pieces were gently agitated in the digestion solution with tweezers to release the protoplasts. The mixture was filtered through a fine mesh (100 mesh) to remove undigested leaf debris. The samples were then centrifuged at 600 rpm for 3 min, and the supernatant was discarded, followed by the completion of subsequent protoplast imaging within 2–3 h. The resulting precipitate was kept in the dark and treated with 1 μL of Hoechst dye for a staining duration of 30 s to 1 min. Following staining, immediate centrifugation at 600 rpm for 3 min was performed, after which the supernatant was removed, and 2 mL of clean liquid was added. Another round of centrifugation at 600 rpm for 3 min was carried out. The protoplasts were washed two to three times, leaving approximately 200 μL of liquid for resuspension. Finally, the prepared protoplasts were mounted onto a slide (Rolland, 2018). Observation under a fluorescence microscope (*Olympus* IX73) was conducted using white light and green fluorescence (emission wavelength 510–540 nm). The protoplasts of WT plants served as the control group.

Observation of subcellular localization through transient transformation of onion epidermal cells: The lower epidermis of fresh onions, measuring 1 × 1 cm, was aseptically excised using sterile tweezers and a scalpel on a laminar flow bench. Subsequently, the excised tissues were carefully placed onto solid 1/2 MS medium in Petri dishes. The dishes were then hermetically sealed with adhesive film and paper tape, wrapped with newspaper for additional protection, and finally incubated at 28°C for 24 h. The *Agrobacterium* (GV3101) carrying the 35S::*BnaBnaBPA03*-eGFP vector and the *Agrobacterium* (GV3101) carrying the 35S::eGFP vector were cultured until reaching an OD600 value of approximately .8. Subsequently, they were centrifuged, resuspended, and mixed with equally treated *Agrobacterium* (EHA105) containing the pSoup-p19 vector, respectively. The mixed *Agrobacterium* solution was utilized for a 30-min infection of the previously cultured onion lower epidermis. Subsequently, the infected onion lower epidermis was transferred onto a solid 1/2 MS medium and sealed in a petri dish, followed by incubation at 28°C for 48 h (Xu et al., 2014). Observation under a fluorescence microscope was conducted using white light and green fluorescence (emission wavelength 510–540 nm). 35S::eGFP was used as the control group.

2.5 | Extraction of total RNA and detection using RT qPCR

According to the experimental requirements, tissue samples were selected from various parts of rapeseed (including root, stem, leaf, flower, bud, inflorescence tip, pedicel, and silique pericarp) at different developmental stages. Subsequently, these samples were rapidly frozen in liquid nitrogen and subsequently pulverized using a pestle. Total RNA was extracted utilizing the TRLzol kit (Invitrogen, Carlsbad, CA). According to the manufacturer's instructions (Vazyme), 1000 ng of total RNA was reverse-transcribed into a 20 μL cDNA using the HiScript III RT SuperMIX for qPCR (+gDNA wiper) kit, which served as a template for subsequent RT qPCR analysis. The RT qPCR was performed with SYBR Green I supermix (Vazyme) according to the manufacturer's instructions. The relative expression levels were calculated using the $2^{-\Delta\Delta CT}$ method and expressed as the relative quantity of target normalized to the reference gene *BnaActin7*

(*BnaC02G0032400XY*) from *B. napus*. In this study, flower tissue was used as the control group when measuring the expression levels of *BnaBPA03* and *BnaBPC03* in various tissues, while other RT qPCR analyses utilized the WT as the control group. Primers used for RT qPCR are listed in Table S1. All quantitative analyses were performed on three independent biological replicates.

2.6 | Detection of ethylene and gibberellin levels

Fresh samples weighing .5 ~ 1 g were measured, and their weights were recorded. Subsequently, ice bath homogenization (or liquid nitrogen grinding) was performed by adding 9 mL of PBS (pH = 7.2 ~ 7.4, .01 mol/L). The resulting mixture was then centrifuged at 5000 ×***g*** for 15 min, and the supernatant was collected as the sample for further analysis. According to the instructions provided by Giled Biotechnology Company for the Plant Ethylene (ETH) ELISA kit and Plant Gibberellin (GA) ELISA kit, a standard curve was constructed using the provided standard samples. Sample wells were designated for testing, while blank controls were prepared without adding any samples or enzyme-labeled reagents. The absorbance of each well was measured at a wavelength of 450 nm with the blank control for zeroing. The remaining steps were unchanged. For the determination of ethylene and gibberellin levels in *bp2-11* and WT plants, the provided sample dilution solution from the kit was utilized to perform onefold and fivefold dilutions on the tested samples. Subsequently, only those diluted samples with absorbance values falling within the range of standard curve were selected for statistical analysis. All analyses were conducted using three biological replicates, and statistical analysis was performed using a *t*-test followed by data visualization in GraphPad Prism 8.

2.7 | Assessment of phenotypic characteristics

The phenotypic analysis was conducted on T2 generation plants cultivated in a controlled temperature environment. During the period when the plants were about to bolt, statistical analysis was performed on leaf angle and stem length. Flowering observations were made at three time points: Week 7, Weeks 8–9, and Week 10, with the number of true leaves recorded at the time of bolting. These experiments involved phenotypic observation and statistical analysis of three independently grown batches of plants. In each independent batch, three WT plants were used as controls, and data from three plants were collected for each plant line.

When analyzing petal shedding, the number of flowers produced by each plant was recorded post-flowering. Statistical analysis was conducted on the number of flowers produced by three independent groups: WT plants, mutant plants, and overexpressed plants, until all petals had fallen from the WT group. Data from three plants were collected for each plant line.

For the determination of seed germination, mature seeds from mutant and WT plants were carefully selected, excluding any withered or stunted seeds. Subsequently, 30 seeds from both mutant and WT groups were systematically arranged on moist filter paper placed on a 120 mm glass plate and cultured at a temperature of 22°C in darkness. Germination was deemed to have occurred upon radicle emergence from the seed coat. The germination rate was recorded at 3-h intervals, commencing from 0 h. Three independent batches of experiments were conducted for data collection. The original data were sorted, and GraphPad Prism 8 and Office software were utilized for the analysis of the phenotypic data. Adobe Illustrator software was employed to organize the figures.

3 | RESULTS

3.1 | The protein sequences of BnaBP and AtBP show similarity and share a very close evolutionary relationship

To investigate the functionality of *BnaBP*, we utilized the BnGDXY database (https://yanglab.hzau.edu.cn/index/vir/index_two.1) to obtain two homologous genes: *BnaBPA03* (*BnaA03G0253200XY*) and *BnaBPC03* (*BnaC03G0290900XY*) in *B. napus*. Their CDS sequences exhibit a variation of 17 bases, resulting in six amino acid disparities within the translated protein sequence. The open reading frame length for both sequences is 1164 bp, encoding 387 amino acids. Furthermore, their protein sequences demonstrate a similarity of 87.97% and 87.22%, respectively, compared to the AtBP protein in Arabidopsis (Figure 1a). The results of gene structure and protein conserved domain analysis revealed that the *AtBP* gene exhibited a similar structural pattern to the *BnaBPA03* and *BnaBPC03* genes. Notably, their protein sequences encompassed KNOX I, KNOX II, ELK, and HOX domains, which are hallmark features of the KNOX protein family (Figure 1b).

KNOX proteins from Arabidopsis, rice, and *B. napus* were subjected to phylogenetic analysis. The results demonstrate that BnaBPA03 and BnaBPC03 exhibit a close genetic relationship with AtBP (AT4G08150), OSH15 (Os07g0129700), and Oskn1 (Os03g0727000), indicating their classification as members of the Class I KNOX protein family (Figure 2).

3.2 | *BnaBP* exhibits high expression in the stem, root, and flower, with subcellular localization in the nucleus

To investigate the expression patterns of *BnaBP* in various tissues of *B. napus*, we used RT qPCR to measure the expression levels of *BnaBPA03* and *BnaBPC03*. The results revealed significant differential expression of *BnaBPA03* and *BnaBPC03* in seven tissue compartments, with the highest expression observed in the stem, followed by the pedicel, root, and flower. Then, we observed lower levels of expression in the inflorescence tip, bud, and silique pericarp; intriguingly, minimal to no expression was detected in leaves (Figure 3a). To determine the subcellular localization of BnaBP, we stably

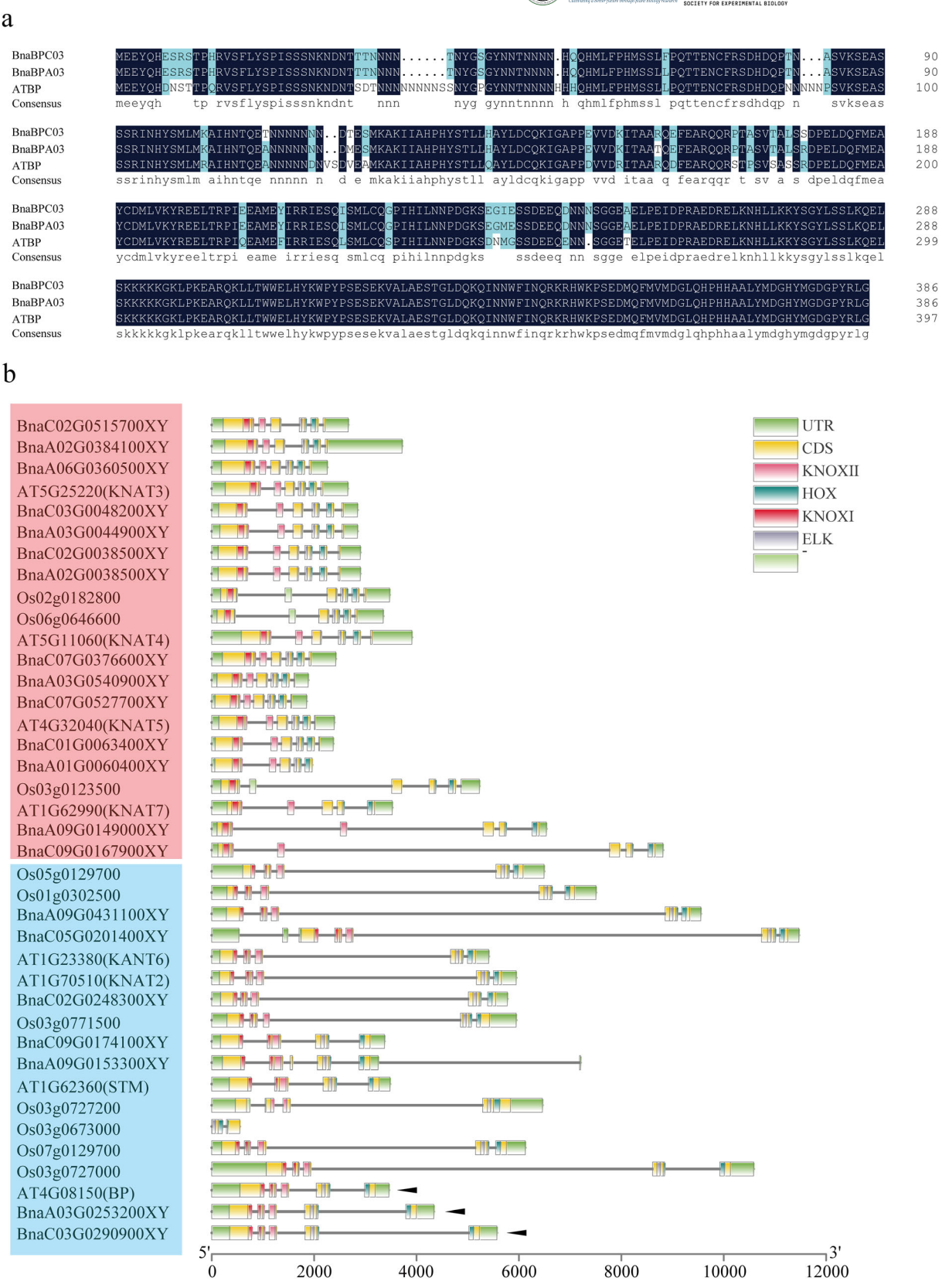

FIGURE 1 Conserved domain analysis of the KNOX protein. (a) Comparison of BnaBPA03, BnaBPC03, and Arabidopsis AtBP protein sequences. (b) Gene structure analysis and identification of conserved domains of KNOX proteins in *Brassica napus*, *Oryza sativa*, and Arabidopsis. The red portion represents Class II KNOX, while the blue segment corresponds to Class I KNOX. The gene structure and protein conserved domain diagrams of *AtBP*, *BnaBPA03*, and *BnaBPC03* are indicated by black arrows.

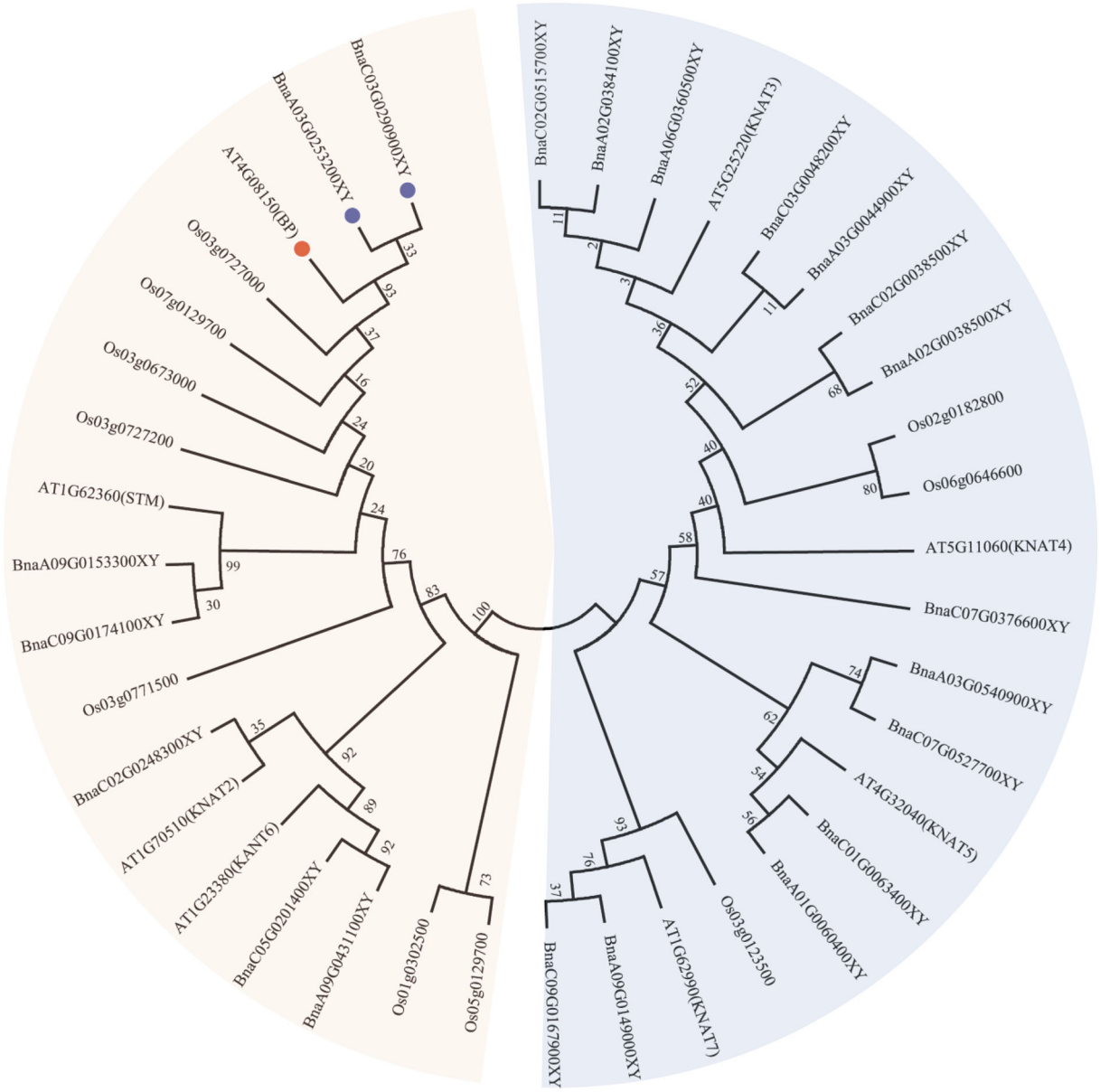

FIGURE 2 Phylogenetic analysis of KNOX proteins in *Brassica napus*, *Oryza sativa*, and Arabidopsis. The protein sequences of a total of 39 samples were subjected to multiple sequence alignments using the MUSCLE algorithm with default parameters. Subsequently, a phylogenetic tree was constructed based on maximum likelihood analysis using MEGA 5 software. The orange segment represents the Class I KNOX protein family, while the blue segment corresponds to the Class II KNOX protein family. The aligned BP proteins originating from Arabidopsis and *B. napus* are marked by round shapes.

transformed the 35S::*BnaBPA03*-eGFP vector into rapeseed and obtained positive transformed plants. Leaf protoplasts were isolated and used to prepare temporary slides for microscopic analysis. The subcellular localization of *BnaBPA03* was observed under a fluorescence microscope, with WT rapeseed leaf protoplasts serving as negative controls. The fluorescence signal and Hoechst staining regions were observed to overlap, providing evidence for the nuclear localization of BnaBP (Figure 3b). This finding was further corroborated through subcellular localization experiments conducted on the lower epidermis of onion (Figure S3).

3.3 | Identification of knockout plants and overexpression plants

To further investigate the specific functions of *BnaBPA03* and *BnaBPC03*, we utilized the CRISPR/Cas9 system to knock out these two genes. During this process, we also noted an interesting observation: In the T0 generation of plants transformed with the CRISPR vector, it is sometimes observed that a single gene (either the *BnaBPA03* gene or the *BnaBPC03* gene) exhibits different types of edits within a single plant. This may result from the two alleles undergoing different

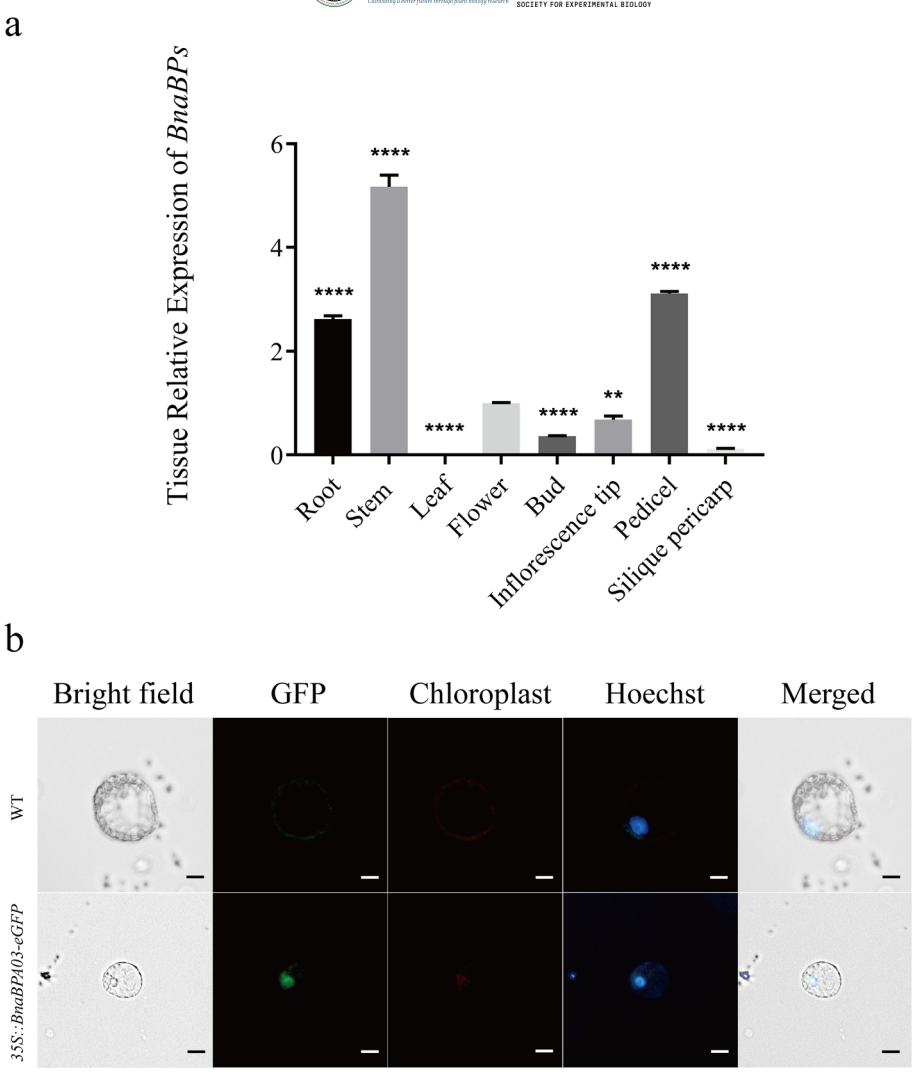

FIGURE 3 Expression analysis of *BnaBPs*. (a) Expression pattern of *BnaBPs* in various tissues. Using BnaBP-QF/R primers, both *BnaBPA03* and *BnaBPC03* were targeted simultaneously. One-way analysis of variance (ANOVA) was conducted to test the mean differences between each tissue and the control group (flower). ANOVA results: $F(7, 16) = 13$, $p < .0001$. Flower was used as the control group, and the data were analyzed post hoc using Dunnett's test. Error bars represent ±SD. Significant levels: ****$p < .0001$, **$p < .01$. (b) Subcellular localization of BnaBPA03. In the figure, green indicates the expression of BnaBPA03 fused with GFP, while blue represents the cell nuclei. The protoplasts were derived from the true leaves of 4-week-old T2 generation plants. This plant line was obtained from plants that had been stably transformed with the 35S::*BnaBPA03*-eGFP vector. Bar = 20 μm.

types of editing. Furthermore, we also speculate that the plant may have developed from more than one cell, with these cells exhibiting different editing types of the *BnaBPA03* and *BnaBPC03* genes. This requires further exploration. In the subsequent screening process for plants with stable editing types, a total of six plant lines with edits at the target sites of both *BnaBPA03* and *BnaBPC03* were obtained, and stable T1 generation plants with edited types were produced through self-pollination (Figure S1). In one of the plant lines, a deletion of the nucleotide sequence between the two target sites of the *BnaBPA03* gene was observed. In the *BnaBPC03* gene, one adenine base was knocked out at target site 2, and one cytosine base was inserted at target site 4. This resulted in frameshift mutations in both *BnaBPA03* and *BnaBPC03*, leading to the premature appearance of stop codons. After editing, the protein lengths of BnaBPA03 and BnaBPC03 were reduced from 387 amino acids to 210 amino acids and 199 amino acids, respectively (Figure S2a–b). Furthermore, from this plant line, we identified a plant that had segregated away the T-DNA insertion. Due to its biallelic mutation and ease of identification, we selected it as the primary subject for subsequent experiments. We designated it as *bp2-11* (Figure S2d). Additionally, we successfully obtained three plants overexpressing *BnaBPA03*, designated as OE-12, OE-15, and OE-16. RT qPCR results indicated that the expression level in the OE-16 plant was the most significant (Figure S2c).

3.4 | The *BnaBP* genes affect flowering time, floral organ abscission, germination, and plant architecture in *B. napus*

Observations of the *bp2-11* and OE-16 plants revealed that *bp2-11* exhibited an early bolting and flowering phenotype compared to the WT (Figure 4a–b). Using the time of the first flower as a measure of flowering time, *bp2-11* flowered approximately 1 week earlier than WT, while OE-16 flowered 3 to 4 weeks later, indicating significant differences (Figure 4c–d). Additionally, *bp2-11* displayed accelerated seed germination (Figure 4e). Corresponding to the earlier flowering time, *bp2-11* was also associated with more easily shed petals, whereas OE-16 exhibited reduced petal abscission (Figure 4f–g). These observations align with previous findings reported by Shi et al. (2011) and Geng et al. (2022). Alterations in leaf angle and stem length were also observed in the *bp2-11* and OE-16 plants. The *bp2-11* plants exhibited an increased blade angle (Figure 4h–i) and

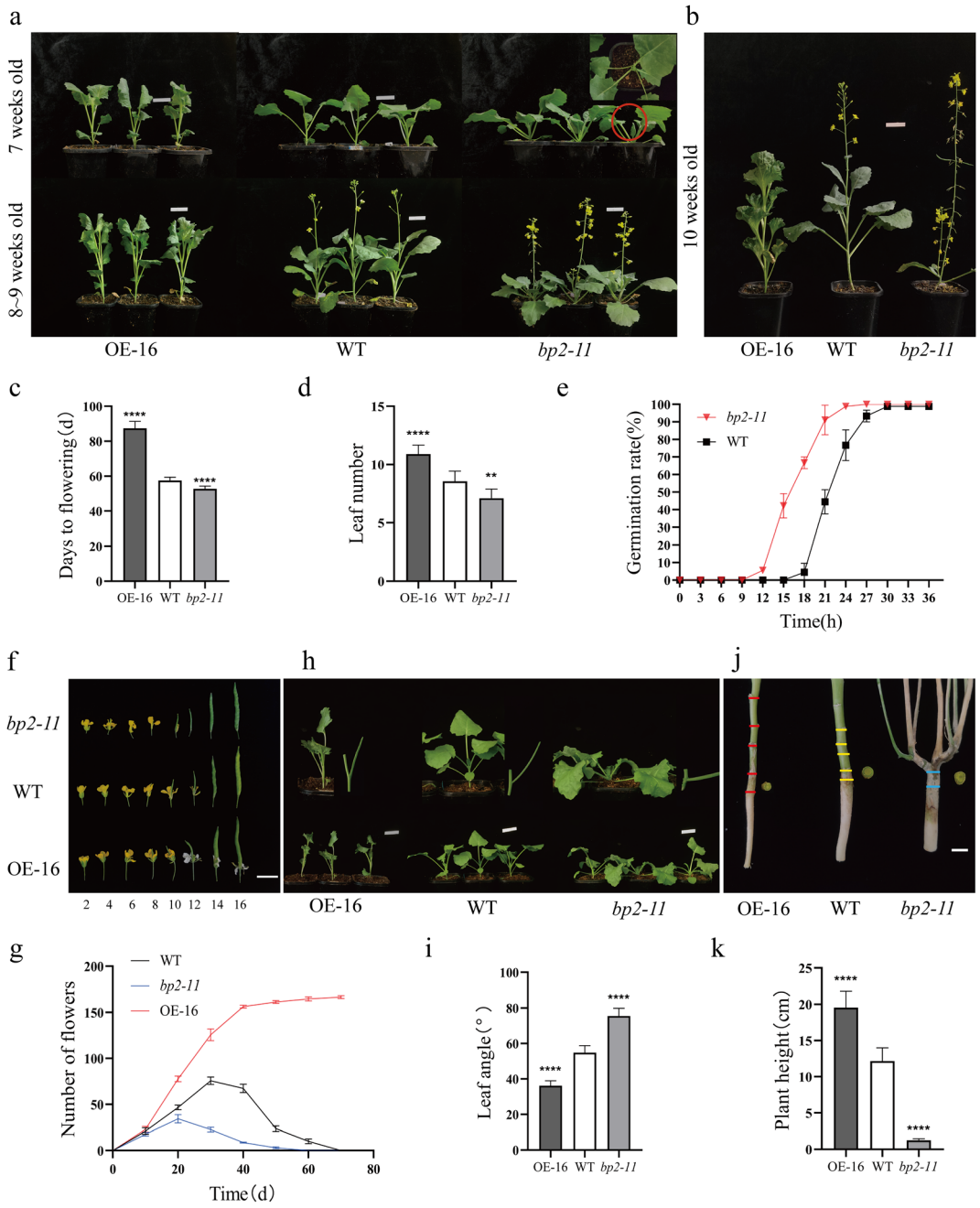

FIGURE 4 Phenotypic evaluation. (a–d) Observation of flowering in rapeseed at 7 to 10 weeks and statistical analysis of flowering time. The red box indicates that the *bp2-11* plants have begun to bolt, and the number of true leaves was recorded at the onset of bolting for each plant. (e) Statistical analysis of germination of *bp2-11* and wild type (WT) within 0–36 h. The red line represents the seed germination of *bp2-11* plants, while the black line represents that of WT plants. $n = 3$ independent batches, each consisting of 30 seeds. (f–g) Floral organ abscission after anthesis in OE-16, WT, and *bp2-11*. The number of flowers produced by each plant was recorded post-flowering until all petals had fallen from the wild-type group. $n = 3$ plant samples. (h–i) Observation and statistical analysis of leaf angles. The measurement of leaf angles was conducted when the plants were approaching the bolting stage. (j) Observation of stem and hypocotyl morphology. The red and yellow lines represent the positional progression from the cotyledon to the fourth true leaf of the plant. Meanwhile, the blue line illustrates the developmental trajectory of the *bp2-11* from its cotyledon to its upper sect stem. (k) Statistics on midsection stem length during the bolting stage of OE-16, WT, and *bp2-11*. In (c,d,i,k), $n = 9$ plant samples. In (a,b,h), Bar = 5 cm. In (f), Bar = 2 cm. In (j), Bar = .5 cm. Error bars represent ±SD. Asterisks indicate a significant difference (Student's *t*-test: $^{**}p < .01$, $^{****}p < .0001$).

droopy horn fruit, while OE-16 displayed a decreased blade angle. Additionally, compared to WT, *bp2-11* showed shorter and thicker stems, resulting in reduced stem spacing that caused almost overlapping true leaf petioles, as well as transverse thickening of the epicotyl and hypocotyl (Figure 4j-k). The observed variations in stem, epicotyl, and hypocotyl align with the classic triple response to

ethylene. Conversely, in OE-16 plants, there was an increase in stem spacing, leading to longer stem lengths (Figure 4j). Furthermore, along with the increased leaf angle phenotype, *bp2-11* exhibited concentrated stems and expanded horizontal leaf area. In contrast, OE-16 demonstrated a phenotype characterized by reduced leaf angle and a more compact plant architecture. Phenotypic observations and statistical analyses of the knockout plant *bp1-11-6* and the overexpressed plant OE-12 further substantiated the impact of *BnaBP* on the phenotype of *B. napus* (Figure S4).

3.5 | *BnaBP* influences the expression of ethylene and gibberellin biosynthesis-related genes as well as flowering-related genes

Previous studies have demonstrated that the *KNOX* gene exerts direct regulatory control over genes involved in ethylene and GA synthesis in plants, thereby influencing the levels of these phytohormones (Sakamoto et al., 2001; Zhao et al., 2020). These two phytohormones play crucial roles in plant germination, flowering time, and morphological development (Chen, Althiab Almasaud, et al., 2020; Fukazawa et al., 2021; Lin et al., 2020). Consequently, we quantified the expression levels of genes associated with ethylene and GA biosynthesis. The expression levels of ethylene-synthesizing genes *BnaACS1*, *BnaACS7*, *BnaACO2*, GA-synthesizing gene *BnaGA20ox*, as well as floral integrators *BnaFT* and *BnaSOC1*, were found to be upregulated in the *bp2-11* mutant plant (Figure 5). These results indicate that the expression of GA, ethylene, and flowering-promoting genes is regulated by the *BnaBPA03* and *BnaBPC03* genes. Meanwhile, the ethylene and GA levels of 7-week-old rapeseed were quantified using ELISA, revealing an increase in both ethylene and GA levels upon knockout of the *BnaBPA03* and *BnaBPC03* genes (Figure S4k). We propose that the *BnaBPA03* and *BnaBPC03* genes may regulate flowering by modulating the expression of the *BnaFT* and *BnaSOC1* genes. Additionally, it exerts an influence on the expression of genes associated with ethylene and GA synthesis, thereby inducing alterations in ethylene and GA levels.

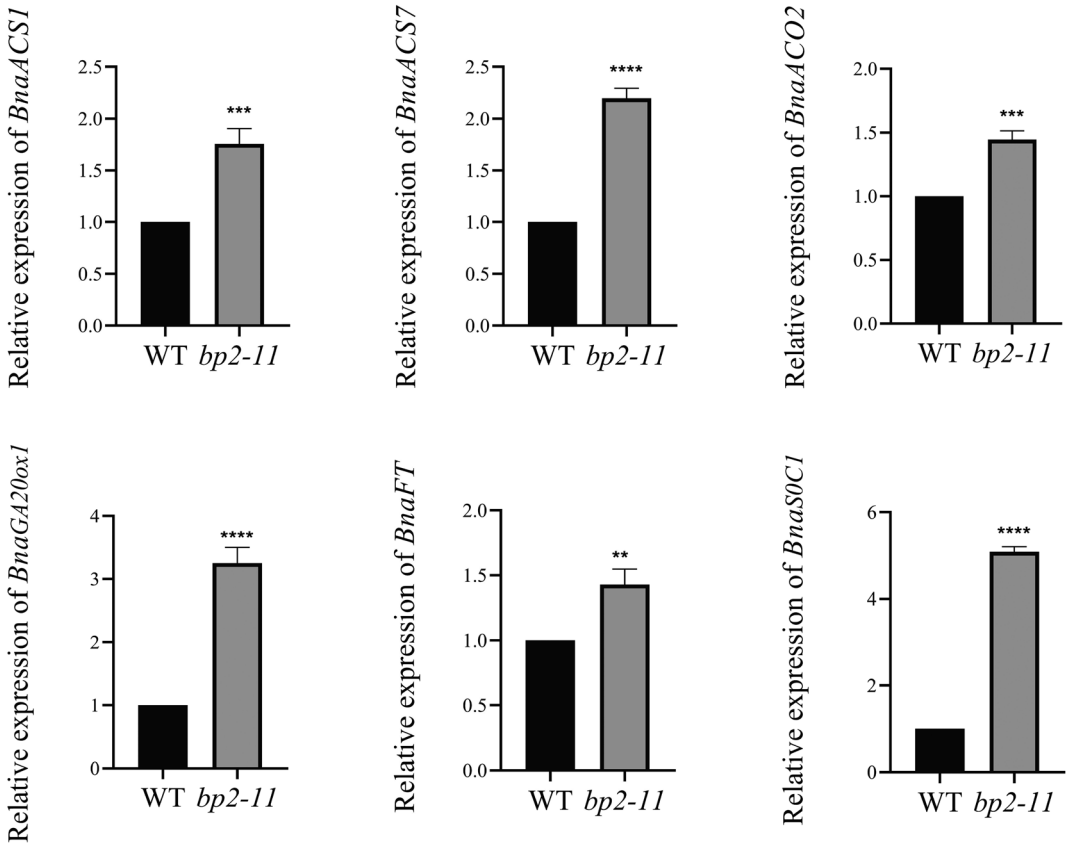

FIGURE 5 Alterations in the expression patterns of genes associated with gibberellin and ethylene biosynthesis, as well as flowering, were observed in *bp2-11*. The relative expression levels were calculated using the $2^{-\Delta\Delta CT}$ method and expressed as the relative quantity of the target normalized to the reference gene *BnaActin7* (*BnaC02G0032400XY*) from *Brassica napus*. *BnaACS1*, *BnaACS7*, *BnaACO2*, *BnaGA20ox1*, *BnaFT*, and *BnaSOC1* represent the 1-aminocyclopropane-1-carboxylate synthase1/7 gene, 1-aminocyclopropane-1-carboxylate oxidase gene, gibberellin 20 oxidase 1 gene, *FLOWERING LOCUS T*, and *SUPPRESSOR OF OVEREXPRESSION OF CONSTANS1* gene in *B. napus*, respectively. See Table S2 for detailed gene IDs. The expression levels of *BnaACS1*, *BnaACS7*, *BnaACO2*, and *BnaGA20ox1* were quantified using RNA extracted from the aboveground tissues of 3- to 4-week-old *B. napus* seedlings. Meanwhile, the expression levels of *BnaFT* and *BnaSOC1* were assessed using RNA isolated from the leaves of 7-week-old *B. napus*. Error bars represent ±SD. Asterisks indicate a significant difference (Student's *t*-test: $^{**}p < .01$, $^{***}p < .001$, $^{****}p < .0001$).

4 | DISCUSSION

Flowering time and plant architecture are pivotal attributes of plants. Flowering time significantly influences the growth cycle of plants, serving as an adaptive strategy for plants to cope with diverse climatic conditions and pollination pressures. The morphology of plants plays a pivotal role in facilitating optimal crop density and enhancing photosynthetic efficiency (Donald, 1968; Wang et al., 2018). The *KNOX* gene family, belonging to the three-amino-acid loop extension (TALE) superfamily, plays a pivotal role in various aspects of plant growth and development (Magnani & Hake, 2008). The *BP* gene, a member of the Class I *KNOX* gene family, has been extensively studied in Arabidopsis (Lincoln et al., 1994), rice (Yoon et al., 2017), and other plant species due to its crucial role in plant growth and development as well as in plant architecture. The *BnaBPA03* and *BnaBPC03* clones obtained in this study exhibit significant similarity to *AtBP* in terms of gene structure and protein sequence, with high expression levels observed in stems, roots, pedicels, and flowers. Additionally, the BnaBPA03 protein is localized in the nucleus. Overexpression and knockout of *BnaBP* demonstrated the regulatory role of *BnaBP* in controlling flowering time, floral organ abscission, and leaf angle, as well as its impact on ethylene and GA levels. Therefore, it is imperative to investigate the molecular functionality of the *BnaBP* gene to enhance plant architecture and optimize flowering time in *B. napus*.

The architecture of the plant and the flowering time of *B. napus* are regulated by multiple factors, with GA playing a pivotal role in orchestrating these processes. In Arabidopsis, GA has been demonstrated to play an indispensable role in the regulation of flowering (Wilson et al., 1992). Endogenous GA promotes flowering by suppressing the expression of *EARLY FLOWERING3* (*ELF3*), *SHORT VEGETATIVE PHASE* (*SVP*), *TEMPRANILLO 1* (*TEM1*), and *TEM2*, which are known inhibitors of flowering. Consequently, this upregulates the expression of two key floral integrators, *FT* and *SOC1* (Fukazawa et al., 2021). In our experimental findings, *BnaBPA03* and *BnaBPC03* knockout plants exhibited an accelerated flowering time of approximately 1 week compared to the WT. In contrast, overexpressed plants showed a delayed flowering time of two to 3 weeks. Furthermore, the knockout plants demonstrated an early germination phenotype. Sakamoto et al. (2001) demonstrated the inhibitory role of KNOX homologous domain proteins in the regulation of GA biosynthesis gene expression, thus modulating GA content. We determined the expression of *GA20ox*, a gene associated with GA synthesis. Compared to the WT, *BnaBPA03* and *BnaBPC03* knockout plants exhibited simultaneous upregulation of *GA20ox1*, a crucial gene involved in gibberellin synthesis, as well as two downstream floral integration genes, *FT* and *SOC1* (Wang et al., 2016). Additionally, these plants displayed relatively high levels of gibberellins. These findings suggest that *BnaBP* may exert a negative regulatory effect on *GA20ox1* expression and gibberellin levels. Furthermore, *BnaBP* can also influence the expression of *FT* and *SOC1*, leading to early flowering. Similarly, we also observed the impact of *BnaBP* on leaf angle. *BnaBPA03* and *BnaBPC03* knockout plants exhibited an increased leaf angle, whereas overexpressed plants displayed a decreased leaf angle. The observed phenomenon was concomitant with an upregulation of *GA20ox1* expression and an increase in leaf angle, which aligns with the findings reported by Jang et al. (2021). In comparison to the study conducted by Shi et al. (2011) in Arabidopsis, horizontally oriented pedicels were also observed in *B. napus*, suggesting a potential similarity in the regulatory mechanisms underlying the increase in leaf angle.

Knockout and overexpression of the *BnaBP* gene resulted in a diverse range of phenotypic alterations, suggesting its potential to influence plant growth and development through modulation of multiple hormonal pathways or regulatory mechanisms. In the study by Shi et al. (2011), it was determined that *BP* is located downstream of the *IDA-HAE/HSL2*-regulated shedding. The absence of the *BP* gene results in floral organ abscission, which aligns with our observations in *B. napus*. Furthermore, in litchi, *BP* exhibits a direct binding affinity to the promoter regions of the *LcACS* and *LcACO* ethylene biosynthesis genes, resulting in suppression of their expression and consequent inhibition of ethylene production. The overexpression of *LcBP* in tomato resulted in delayed pedunculation and reduced plant sensitivity to ethylene (Zhao et al., 2020). In *B. napus*, the knockout of *BnaBPA03* and *BnaBPC03* resulted in the upregulation of *BnaACS1*, *BnaACS7*, and *BnaACO2* expression, leading to an increase in ethylene levels. These findings suggest that *BnaBP* may exert a negative regulatory effect on the expression of these genes and influence ethylene production. Furthermore, we observed shorter stems and transverse thickening of the epicotyl and hypocotyl, consistent with the classic ethylene triple response, further supporting the notion that *BnaBP* negatively regulates ethylene biosynthesis.

In this study, our experimental findings demonstrate the crucial role of *BnaBP* in regulating flowering time and plant architecture, while also suggesting its involvement in the regulation of ethylene and GA biosynthesis. These results provide a theoretical foundation for further investigations into the biological functions and molecular mechanisms of the *BnaBP* gene in relation to flowering time and plant morphology in rapeseed, offering valuable insights for improving flowering and optimizing plant architecture.

AUTHOR CONTRIBUTIONS

Material preparation, data collection, and analysis were conducted by Jiang Yu and Yi-Xuan Xue. The initial draft of the manuscript was written by Jiang Yu. All authors contributed to the review and revision of earlier versions of the manuscript. Xiao-Li Tan contributed to the research design and manuscript proofreading. All authors have reviewed and approved the final version of the manuscript.

ACKNOWLEDGMENTS

This work was supported by the Jiangsu Agriculture Science and Technology Innovation Fund (CX (21) 2009) and Key R&D in the Jiangsu Province (BE2023342; BE2022340).

CONFLICT OF INTEREST STATEMENT

The authors declare no competing interests.

DATA AVAILABILITY STATEMENT

The datasets generated during and/or analyzed during the current study are available from the corresponding author upon reasonable request.

ORCID

Xiao-Li Tan https://orcid.org/0000-0002-9358-605X

REFERENCES

Beyzi, E., Gunes, A., Buyukkilic Beyzi, S., & Konca, Y. (2019). Changes in fatty acid and mineral composition of rapeseed (*Brassica napus* ssp. *oleifera* L.) oil with seed sizes. *Industrial Crops and Products*, *129*, 10–14. https://doi.org/10.1016/j.indcrop.2018.11.064

Bhalla, P. L., & Singh, M. B. (2008). Agrobacterium-mediated transformation of *Brassica napus* and *Brassica oleracea*. *Nature Protocols*, *3*(2), 181–189. https://doi.org/10.1038/nprot.2007.527

Bueno, N., Alvarez, J. M., & Ordás, R. J. (2020). Characterization of the KNOTTED1-LIKE HOMEOBOX (KNOX) gene family in *Pinus pinaster* Ait. *Plant Science*, *301*, 110691. https://doi.org/10.1016/j.plantsci.2020.110691

Chen, C., Chen, H., Zhang, Y., Thomas, H. R., Frank, M. H., He, Y., & Xia, R. (2020). TBtools: An integrative toolkit developed for interactive analyses of big biological data. *Molecular Plant*, *13*(8), 1194–1202. https://doi.org/10.1016/j.molp.2020.06.009

Chen, Y., Althiab Almasaud, R., Carrie, E., Desbrosses, G., Binder, B. M., & Chervin, C. (2020). Ethanol, at physiological concentrations, affects ethylene sensing in tomato germinating seeds and seedlings. *Plant Science: An International Journal of Experimental Plant Biology*, *291*, 110368. https://doi.org/10.1016/j.plantsci.2019.110368

Cheng, L., Li, R., Wang, X., Ge, S., Wang, S., Liu, X., He, J., Jiang, C. Z., Qi, M., Xu, T., & Li, T. (2022). A SlCLV3-SlWUS module regulates auxin and ethylene homeostasis in low light-induced tomato flower abscission. *Plant Cell*, *34*(11), 4388–4408. https://doi.org/10.1093/plcell/koac254

Donald, C. M. (1968). The breeding of crop ideotypes. *Euphytica*, *17*(3), 385–403. https://doi.org/10.1007/BF00056241

Douglas, S. J., Chuck, G., Dengler, R. E., Pelecanda, L., & Riggs, C. D. (2002). KNAT1 and ERECTA regulate inflorescence architecture in Arabidopsis. *Plant Cell*, *14*(3), 547–558. https://doi.org/10.1105/tpc.010391

Fukazawa, J., Ohashi, Y., Takahashi, R., Nakai, K., & Takahashi, Y. (2021). DELLA degradation by gibberellin promotes flowering via GAF1-TPR-dependent repression of floral repressors in Arabidopsis. *Plant Cell*, *33*(7), 2258–2272. https://doi.org/10.1093/plcell/koab102

Geng, R., Shan, Y., Li, L., Shi, C. L., Zhang, W., Wang, J., Sarwar, R., Xue, Y. X., Li, Y. L., Zhu, K. M., Wang, Z., Xu, L. Z., Aalen, R. B., & Tan, X. L. (2022). CRISPR-mediated BnaIDA editing prevents silique shattering, floral organ abscission, and spreading of Sclerotinia sclerotiorum in *Brassica napus*. *Plant Communications*, *3*(6), 100452. https://doi.org/10.1016/j.xplc.2022.100452

Guo, P., Li, Z., Huang, P., Li, B., Fang, S., Chu, J., & Guo, H. (2017). A tripartite amplification loop involving the transcription factor WRKY75, salicylic acid, and reactive oxygen species accelerates leaf senescence. *Plant Cell*, *29*(11), 2854–2870. https://doi.org/10.1105/tpc.17.00438

Jang, S., Cho, J. Y., Do, G. R., Kang, Y., Li, H. Y., Song, J., Kim, H. Y., Kim, B. G., & Hsing, Y. I. (2021). Modulation of rice leaf angle and grain size by expressing OsBCL1 and OsBCL2 under the control of OsBUL1 promoter. *International Journal of Molecular Sciences*, *22*(15), 7792. https://doi.org/10.3390/ijms22157792

Liao, Z., Yu, H., Duan, J., Yuan, K., Yu, C., Meng, X., Kou, L., Chen, M., Jing, Y., Liu, G., Smith, S. M., & Li, J. (2019). SLR1 inhibits MOC1 degradation to coordinate tiller number and plant height in rice. *Nature Communications*, *10*(1), 2738. https://doi.org/10.1038/s41467-019-10667-2

Lin, Q., Zhang, Z., Wu, F., Feng, M., Sun, Y., Chen, W., Cheng, Z., Zhang, X., Ren, Y., Lei, C., Zhu, S., Wang, J., Zhao, Z., Guo, X., Wang, H., & Wan, J. (2020). The APC/C (TE) E3 ubiquitin ligase complex mediates the antagonistic regulation of root growth and tillering by ABA and GA. *Plant Cell*, *32*(6), 1973–1987. https://doi.org/10.1105/tpc.20.00101

Lincoln, C., Long, J., Yamaguchi, J., Serikawa, K., & Hake, S. (1994). A knotted1-like homeobox gene in Arabidopsis is expressed in the vegetative meristem and dramatically alters leaf morphology when overexpressed in transgenic plants. *The Plant Cell*, *6*(12), 1859–1876. https://doi.org/10.1105/tpc.6.12.1859

Long, J. A., Moan, E. I., Medford, J. I., & Barton, M. K. (1996). A member of the KNOTTED class of homeodomain proteins encoded by the STM gene of Arabidopsis. *Nature*, *379*(6560), 66–69. https://doi.org/10.1038/379066a0

Lu, K., Wei, L., Li, X., Wang, Y., Wu, J., Liu, M., Zhang, C., Chen, Z., Xiao, Z., Jian, H., Cheng, F., Zhang, K., Du, H., Cheng, X., Qu, C., Qian, W., Liu, L., Wang, R., Zou, Q., … Li, J. (2019). Whole-genome resequencing reveals *Brassica napus* origin and genetic loci involved in its improvement. *Nature Communications*, *10*(1), 1154. https://doi.org/10.1038/s41467-019-09134-9

Magnani, E., & Hake, S. (2008). KNOX lost the OX: The Arabidopsis KNATM gene defines a novel class of KNOX transcriptional regulators missing the homeodomain. *Plant Cell*, *20*(4), 875–887. https://doi.org/10.1105/tpc.108.058495

Meir, S., Philosoph-Hadas, S., Sundaresan, S., Selvaraj, K. S., Burd, S., Ophir, R., Kochanek, B., Reid, M. S., Jiang, C. Z., & Lers, A. (2010). Microarray analysis of the abscission-related transcriptome in the tomato flower abscission zone in response to auxin depletion. *Plant Physiology*, *154*(4), 1929–1956. https://doi.org/10.1104/pp.110.160697

Ragni, L., Belles-Boix, E., Günl, M., & Pautot, V. (2008). Interaction of KNAT6 and KNAT2 with BREVIPEDICELLUS and PENNYWISE in Arabidopsis inflorescences. *Plant Cell*, *20*(4), 888–900. https://doi.org/10.1105/tpc.108.058230

Rolland, V. (2018). Determining the subcellular localization of fluorescently tagged proteins using protoplasts extracted from transiently transformed *Nicotiana benthamiana* leaves. *Methods in Molecular Biology (Clifton, NJ)*, *1770*, 263–283. https://doi.org/10.1007/978-1-4939-7786-4_16

Sakamoto, T., Kamiya, N., Ueguchi-Tanaka, M., Iwahori, S., & Matsuoka, M. (2001). KNOX homeodomain protein directly suppresses the expression of a gibberellin biosynthetic gene in the tobacco shoot apical meristem. *Genes & Development*, *15*(5), 581–590. https://doi.org/10.1101/gad.867901

Shi, C. L., Stenvik, G. E., Vie, A. K., Bones, A. M., Pautot, V., Proveniers, M., Aalen, R. B., & Butenko, M. A. (2011). Arabidopsis class I KNOTTED-like homeobox proteins act downstream in the IDA-HAE/HSL2 floral abscission signaling pathway. *Plant Cell*, *23*(7), 2553–2567. https://doi.org/10.1105/tpc.111.084608

Song, Y. H., Ito, S., & Imaizumi, T. (2010). Similarities in the circadian clock and photoperiodism in plants. *Current Opinion in Plant Biology*, *13*(5), 594–603. https://doi.org/10.1016/j.pbi.2010.05.004

Tamura, K., Peterson, D., Peterson, N., Stecher, G., Nei, M., & Kumar, S. (2011). MEGA5: Molecular evolutionary genetics analysis using maximum likelihood, evolutionary distance, and maximum parsimony methods. *Molecular Biology and Evolution*, *28*(10), 2731–2739. https://doi.org/10.1093/molbev/msr121

Taylor, J. E., & Whitelaw, C. A. (2001). Signals in abscission. *The New Phytologist*, *151*(2), 323–339. https://doi.org/10.1046/j.0028-646x.2001.00194.x

Wang, B., Smith, S. M., & Li, J. (2018). Genetic regulation of shoot architecture. *Annual Review of Plant Biology*, *69*, 437–468. https://doi.org/10.1146/annurev-arplant-042817-040422

Wang, H., Pan, J., Li, Y., Lou, D., Hu, Y., & Yu, D. (2016). The DELLA-CONSTANS transcription factor cascade integrates gibberellic acid and photoperiod signaling to regulate flowering. *Plant Physiology*, *172*(1), 479–488. https://doi.org/10.1104/pp.16.00891

Wang, P., Song, Y., Xie, Z., Wan, M., Xia, R., Jiao, Y., Zhang, H., Yang, G., Fan, Z., Yang, Q. Y., & Hong, D. (2024). Xiaoyun, a model accession for functional genomics research in *Brassica napus*. *Plant Communications*, *5*(1), 100727. https://doi.org/10.1016/j.xplc.2023.100727

Wilson, R. N., Heckman, J. W., & Somerville, C. R. (1992). Gibberellin is required for flowering in *Arabidopsis thaliana* under short days. *Plant Physiology*, *100*(1), 403–408. https://doi.org/10.1104/pp.100.1.403

Xing, H. L., Dong, L., Wang, Z. P., Zhang, H. Y., Han, C. Y., Liu, B., Wang, X. C., & Chen, Q. J. (2014). A CRISPR/Cas9 toolkit for multiplex genome editing in plants. *BMC Plant Biology*, *14*, 327. https://doi.org/10.1186/s12870-014-0327-y

Xu, K., Huang, X., Wu, M., Wang, Y., Chang, Y., Liu, K., Zhang, J., Zhang, Y., Zhang, F., Yi, L., Li, T., Wang, R., Tan, G., & Li, C. (2014). A rapid, highly efficient and economical method of agrobacterium-mediated in planta transient transformation in living onion epidermis. *PLoS ONE*, *9*(1), e83556. https://doi.org/10.1371/journal.pone.0083556

Ye, Z., & Liu, Y. (2023). Polyphenolic compounds from rapeseeds (*Brassica napus* L.): The major types, biofunctional roles, bioavailability, and the influences of rapeseed oil processing technologies on the content. *Food Research International*, *163*, 112282. https://doi.org/10.1016/j.foodres.2022.112282

Yoon, J., Cho, L. H., Antt, H. W., Koh, H. J., & An, G. (2017). KNOX protein OSH15 induces grain shattering by repressing lignin biosynthesis genes. *Plant Physiology*, *174*(1), 312–325. https://doi.org/10.1104/pp.17.00298

Zhao, M., Li, C., Ma, X., Xia, R., Chen, J., Liu, X., Ying, P., Peng, M., Wang, J., Shi, C. L., & Li, J. (2020). KNOX protein KNAT1 regulates fruitlet abscission in litchi by repressing ethylene biosynthetic genes. *Journal of Experimental Botany*, *71*(14), 4069–4082. https://doi.org/10.1093/jxb/eraa162

SUPPORTING INFORMATION

Additional supporting information can be found online in the Supporting Information section at the end of this article.

How to cite this article: Yu, J., Xue, Y.-X., Sarwar, R., Wei, S.-H., Geng, R., Zhang, Y.-F., Mu, J.-X., & Tan, X.-L. (2024). The *BnaBPs* gene regulates flowering time and leaf angle in *Brassica napus*. *Plant Direct*, *8*(10), e70018. https://doi.org/10.1002/pld3.70018